



Mononuclear and dinuclear heteroleptic Cu(I) complexes based on pyridyl-triazole and DPEPhos with long-lived excited-state lifetimes

Claudia Bizzarri ^{a, *}, Andreas P. Arndt ^b, Stephan Kohaut ^c, Karin Fink ^c, Martin Nieger ^d

^a Institute of Organic Chemistry, Karlsruhe Institute of Technology, Fritz-Haber-Weg 6, 76131, Karlsruhe, Germany

^b Light Technology Institute, Karlsruhe Institute of Technology, Karlsruhe, Germany

^c Institute of Nanotechnology, Karlsruhe Institute of Technology, Karlsruhe, Germany

^d Department of Chemistry, University of Helsinki, Helsinki, Finland

ARTICLE INFO

Article history:

Received 28 March 2018

Received in revised form

18 June 2018

Accepted 9 July 2018

Keywords:

Heteroleptic Copper(I) complexes

photosensitizers

carbon dioxide reduction

Ster-Volmer quenching

cooperativity

ABSTRACT

A mononuclear and two dinuclear heteroleptic Cu(I) complexes have been successfully prepared, using the chelating bis [(2-diphenylphosphino)phenyl] ether (DPEPhos) and pyrid-2'-yl-1H-1,2,3-triazole as N'N chelating ligands. They show good luminescence in solution at room temperature with long-lived excited states. Furthermore, bimolecular quenching experiments of these new complexes with the catalyst Ni(cyclam)Cl₂ encourage the use of such compounds as photosensitizers for the photoreduction of carbon dioxide.

© 2018 Elsevier B.V. All rights reserved.

1. Introduction

Nowadays the reduced availability of materials and their recyclability are raising enormous interest in the research community. Furthermore, the exploitation of environmentally sustainable – so called 'green' – resources has become very important. Light can be considered a 'green' reagent; definitely when it comes directly from the sun, but also if it comes from artificial sources. Photons are 'green' in view of the fact that they do not leave any waste products [1].

The development of molecules that can absorb electromagnetic radiation to deliver a certain function is thus a central research question. In particular, photosensitizers based on organometallic complexes [2] have shown promising results in diverse catalytic reactions [3–6] as well as in solar energy conversion [7–9]. Copper(I) complexes represent an appealing alternative to expensive photosensitizers based on ruthenium (II), iridium (III) or rhenium(I) [10,11]. In fact, copper is more abundant in the earth's crust and is therefore cheaper. Moreover, Cu(I) complexes are of easy preparation. Being a *d10* nucleus, metal centred electronic transitions

cannot occur and the excited state of a copper(I) complex is normally a metal-to-ligand charge-transfer state (MLCT). Nevertheless, in the excited state they suffer from a Jahn–Teller flattening distortion from the pseudo-tetrahedral geometry in the ground state, which allows Lewis bases to form adducts and to deactivate the excited state of the copper(I) complex [12,13]. Steric hindrance imposed by the ligands in the coordination sphere avoids this distortion to a certain extent and therefore increases the excited state lifetime and the photoluminescence quantum yield. Lability of the ligands might also complicate the development of such compounds. In fact it has been found that heteroleptic Cu(P'P)(N'N) complexes, where P'P is a chelating diphosphine and N'N is a 1,10-phenanthroline derivative, undergo an exchange of ligands in solution, affording homoleptic Cu(N'N)₂ and Cu(P'P)₂ complexes, which are more favoured [14]. In the solid state, these drawbacks are somehow limited and the utilisation of Cu(I) complexes in light-emitting devices (OLEDs or LEECs) has attracted a strong interest [15–18]. The pioneering work of Sauvage and co-workers with Cu(dap)₂Cl [19] as photoredox catalyst was published in 1987 [20], but apart from some contemporary publications [21], only recently have Cu(I) complexes been applied as photoredox catalysts or photosensitizers (PS) [22–32]. In artificial photosynthesis [33,34] the photosensitizer absorbs the luminous radiation and transfers

* Corresponding author.

E-mail address: claudia.bizzarri@kit.edu (C. Bizzarri).

the energy to a catalyst, which then activates the small molecule (usually either water or carbon dioxide). The characteristics that a PS should have are the following: good absorption in the visible light region, long-lived excited state, and high stability. There are still very few Cu(I)-based PS applied to artificial photosynthesis; nevertheless, they are quite promising [35–40]. We are interested in the development of new PS based on copper(I), which can be used in the homogeneous reduction of CO₂. In this work three heteroleptic Cu(I) coordination compounds based on pyrid-2'-yl-1H-1,2,3-triazole ligand and bis [(2-diphenylphosphino)phenyl] ether (DPEPhos) are presented. The dinuclear complexes have been prepared using the pyrid-2'-yl-1H-1,2,3-triazole as chelating unit, as in mononuclear complex **1H**, bridged by a phenyl ring, substituted in *meta* (**2H**) or in *para* (**3H**) positions. A methyl group *alpha* to the nitrogen atom of the pyridine increases the steric hindrance in the excited state, allowing an increase in the quantum yield in solution of such complexes. In the dinuclear complexes **2H** and **3H**, this effect is more pronounced. The long lifetime of the excited states and their good emission in solution make these complexes very appealing for application as PSs. As a preliminary test, a Stern–Volmer bimolecular quenching experiment was conducted with the three complexes and Ni(cyclam)Cl₂ [41], a known catalyst in the reduction of CO₂ [42].

2. Experimental section

2.1. General information and materials

The starting materials were purchased from commercial suppliers and used without further purification. Solvents for synthesis were purified according standard procedure, if necessary. Dichloromethane was dried over CaH₂ and freshly distilled before each reaction. All air- and water-sensitive experiments were carried out in standard glassware under an inert Ar atmosphere, using standard vacuum line techniques. Tetrakis (acetonitrile)copper(I) tetrafluoroborate was synthesized according to literature procedures.

Warning! Azides and nitrogen-rich compounds can be explosive. Handle with care!

¹H NMR (300 MHz, 500 MHz) and ¹³C{H} NMR (150 MHz) spectra were recorded with a Bruker Avance III spectrometers operating at 298 K in the Fourier transform mode. Chemical shifts are reported in δ units (ppm) using residual CHCl₃ (¹H δ 7.26 ppm, ¹³C δ 77.00) as reference.

2.2. Synthesis

2.2.1. Ligand 1

- (a) *Synthesis 6-methyl-2-phenylethynyl-pyridine*. Under Argon atmosphere, in 20 ml of dry diisopropylamine the reagents were dissolved as following: 2-bromo-6-methylpyridine (1.0 ml, 1.511 g, 8.7 mmol); ethynylbenzene (0.96 ml, 0.897 g, 8.5 mmol). Then the catalyst Pd(PPh₃)Cl₂ (62.2 mg, 0.089 mmol) and the co-catalyst CuI (40.0 mg, 0.21 mmol) were added. The reaction was heated to 80 °C until the starting materials are not present anymore in the reaction mixture (almost after 4 h). A white precipitate was filtered out and the solvent was removed under reduced pressure. The residue was purified by column chromatography in silica gel. Eluent was CH₂Cl₂:C₆H₁₂ (50:50). The product is yellow oil. Yield: 1.2 g (71.3%). ¹H NMR (300 MHz, 298 K, CDCl₃) δ : 7.60–7.55 (m, 2H), 7.51 (d, 1H), 7.36–7.28 (m, 4H), 7.07 (d, 1H), 2.56 (s, 3H).

- (b) *Synthesis 5-(6'-methyl-pyrid-2'-yl)-4-phenyl-1H-1,2,3-triazole*. In 25 ml of dry N,N-dimethylformamide, 6-methyl-2-phenylethynyl-pyridine (1.2 g, 6.2 mmol) was dissolved. Trimethylsilylazide was added (2.5 ml, 2.17 g, 19 mmol) was added and the reaction temperature was set to 110 °C. Trimethylsilylazide was added more than once, so that in total other 20 mmol were added. The reaction stirred for 2 days. The solvent was removed by reduced pressure. The residue was purified by column chromatography in silica with CH₂Cl₂:CH₃OH (98:2) as eluent. A sticky very viscous orange oil was obtained. Yield: 1.105 g, (75%). ¹H NMR (300 MHz, 298 K, CDCl₃) δ : 7.68–7.64 (m, 2H); 7.54 (t, *J*=7.7 Hz, 1H), 7.38 (m, 4H), 7.12 (d, *J*=7.6 Hz, 1H); 2.56 (s, 3H).

2.2.2. Ligand L2

- (a) *Synthesis meta-bis((6'-methyl-pyrid-2'-yl)ethynyl)benzene*. Under Argon atmosphere, in 25 ml of dry diisopropylamine the reagents were dissolved as following: 2-bromo-6-methylpyridine (0.45 ml, 0.678 g, 4.0 mmol); 1,3-diethynylbenzene (0.24 ml, 0.228 g, 1.8 mmol). Then the catalyst Pd(PPh₃)Cl₂ (12 mg, 0.017 mmol) and the co-catalyst CuI (5.2 mg, 0.027 mmol) were added. The reaction was heated to 80 °C until the starting materials are not present anymore in the reaction mixture (almost after 6 h). Solvent was removed under reduced pressure. The residue was dissolved in CH₂Cl₂ and washed with water. The aqueous phases were extracted with 3 \times 10 ml DCM. The organic phases were washed with brine and dried over Na₂SO₄. The residue solvent was removed and the product was purified by column chromatography in silica gel. Eluent was CH₂Cl₂:CH₃OH (99:1). Yield: 0.480 g (88%). ¹H NMR (300 MHz, 298 K, CDCl₃) δ : 7.819 (s, 1H), 7.59 (m, 4H), 7.36 (d, *J*=7.8 Hz, 3H), 7.14 (d, *J*=7.8 Hz, 2H), 2.60 (s, 6H).
- (b) *Synthesis meta-bis(5'-(6''-methyl-pyrid-2''-yl)1H-1,2,3-triazol-4'-yl)benzene*. In 10 ml of N,N-dimethylformamide, *meta-bis*((6'-methyl-pyrid-2'-yl)ethynyl)benzene (0.420 g, 1.36 mmol) was dissolved. Trimethylsilylazide (0.73 ml, 0.633 g, 5.5 mmol) was added and the reaction temperature was set to 110 °C. The reaction stirred for 1 day. The solvent was removed by reduced pressure. The residue was purified by column chromatography in silica with CH₂Cl₂:CH₃OH (98:2) as eluent. Yield: 170 mg, (32%). ¹H NMR (300 MHz, 298 K, CDCl₃) δ : 7.97 (s, 1H); 7.57 (m, 4H), 7.45 (d, *J*=7.8 Hz, 2H), 7.10 (d, *J*=7.6 Hz, 2H); 2.52 (s, 6H).

2.2.3. Ligand L3

- (a) *Synthesis para-bis((6'-methyl-pyrid-2'-yl)ethynyl)benzene*. Under Argon atmosphere, in 10 ml of dry diisopropylamine the reagents were dissolved as following: 2-bromo-6-methylpyridine (99 μ l, 0.15 g, 0.89 mmol); 1,4-diethynylbenzene (0.056 g, 0.44 mmol). Then the catalyst Pd(PPh₃)Cl₂ (2.3 mg, 0.003 mmol) and the co-catalyst CuI (5.1 mg, 0.027 mmol) were added. The reaction was heated to 80 °C until the starting materials are not present anymore in the reaction mixture (almost after 6 h). Solvent was removed under reduced pressure. The residue was dissolved in CH₂Cl₂ and the not soluble fraction was filtered out. The solution was recrystallized by slow evaporation of the solvent. Yield: 0.32 g (72.7%). ¹H NMR (300 MHz, 298 K, CDCl₃) δ : 7.56 (m, 6H); 7.35 (d, 2H); 7.12 (d, 2H); 2.58 (s, 6H).

(b) *Synthesis para-bis(5'-(6''-methyl-pyrid-2''-yl)1H-1,2,3-triazol-4'-yl)benzene*. In 10 ml of *N,N*-dimethylformamide, *para-bis*((6'-methyl-pyrid-2'-yl)ethynyl)benzene (98.6 mg, 0.32 mmol) was dissolved. Sodium azide (184.3 mg, 2.83 mmol) was added and the reaction temperature was set to 110 °C. The reaction stirred for 1 day. The solvent was removed by reduced pressure. The residue was purified by column chromatography in silica with CH₂Cl₂:CH₃OH (95:5) as eluent. Yield: 100 mg, (79.2%). ¹H NMR (300 MHz, 298 K, CDCl₃) δ: 7.76 (4H, broad singlet); 7.60 (t, 2H); 7.165 (d, 2H); 2.61 (s, 6H).

2.2.4. Complex 1H

In a Schlenk tube, under Ar atmosphere, DPEPhos (247.2 mg, 0.46 mmol) and Cu(CH₃CN)₄ BF₄ (148.7 mg, 0.47 mmol) were dissolved in 15 ml of dry and freshly distilled CH₂Cl₂. The reagents stirred for half an hour at room temperature, before the ligand L1 (108.8 mg, 0.46 mmol) was added. The solution became immediately bright yellow. After 4 h, the solvent was evaporated by reduced pressure. The residue was dissolved in a minimum amount of CH₂Cl₂ and recrystallized by slow diffusion of C₆H₁₂. The obtained white crystals were filtrated and dried under vacuum. Yield: 302.5 mg, (71.1%). ¹H NMR (300 MHz, 298 K, CDCl₃) δ: 14.41 (broad s, 1H, NH), 7.75–7.58 (m, 10H), 7.53–7.38 (m, 12H), 7.27–7.25 (m, 5H), 7.13 (m, 4H), 6.98–6.85 (m, 6H), 2.19 (s, 3H). ¹³C NMR (400 MHz, 298 K, CDCl₃) δ: 159.56; 159.50; 159.44; 158.87; 153.04; 144.76; 139.62; 137.72; 136.24; 135.96; 135.52; 133.34; 132.59; 131.83; 130.56; 130.24; 129.797; 129.38; 129.09; 128.98; 127.76; 126.77; 126.65; 126.53; 125.34; 121.46; 121.12; 117.43; 78.29–77.65 (CDCl₃); 26.09. ³¹P NMR (400 MHz, 298 K, CDCl₃) δ: –14.85. HRMS (ESI): 837.20 (*z* = 1) (C₅₀H₄₀CuN₄OP₂⁺). Calcd for C₅₀H₄₀CuN₄OP₂⁺ BF₄⁻: C, 64.91; H, 4.36; N, 6.06. Found: C, 64.67; H, 4.24; N, 6.15.

2.2.5. Complex 2H

In a Schlenk tube, under Ar atmosphere, DPEPhos (193.4 mg, 0.36 mmol) and Cu(CH₃CN)₄ BF₄ (119.1 mg, 0.38 mmol) were dissolved in 20 ml of dry and freshly distilled CH₂Cl₂. The reagents stirred for half an hour at room temperature, before the ligand L2 (70.4 mg, 0.18 mmol) was added. After 6 h, the solvent was evaporated by reduced pressure. The residue was dissolved in a minimum amount of CH₂Cl₂ and recrystallized by slow diffusion of C₆H₁₂. The obtained yellowish-white crystals were filtrated and dried under vacuum. Yield: 420.2 mg, (65.9%). ¹H NMR (400 MHz, 298 K, CDCl₃) δ: 14.41 (broad s, 2H, NH), 8.07 (t, *J* = 7.9 Hz, 2H); 7.76 (t, *J* = 7.8 Hz, 1H); 7.59–7.57 (d, *J* = 8.0 Hz, 2H); 7.53–7.45 (m, 11H), 7.31–7.27 (m, 13H), 7.26 (CHCl₃); 7.24–7.18 (m, 6H); 7.13 (t, *J* = 7.8 Hz, 10H), 6.98–6.92 (m, 8H), 6.78 (m, 8H), 6.68 (m, 4H), 2.01 (s, 6H). ¹³C NMR (400 MHz, 298 K, CDCl₃) δ: 159.496; 159.31; 147.44; 141.57; 141.10; 136.16; 135.55; 135.49; 135.23; 135.06; 133.01; 132.94; 132.78; 132.41; 131.80; 131.49; 131.76; 130.512; 129.68; 129.53; 129.49; 127.36; 125.70; 125.47; 125.36; 121.10; 120.02; 78.24–77.94 (CDCl₃); 26.11. ³¹P NMR (400 MHz, 298 K, CDCl₃) δ: –14.00. HRMS (ESI): 1685.35 (*z* = 1) (C₉₄H₇₄Cu₂N₈O₂P₄BF₄)⁺; 1596.34 (*z* = 2) (C₉₄H₇₄Cu₂N₈O₂P₄H)²⁺. Calcd for C₉₄H₇₄Cu₂N₈O₂P₄H²⁺ 2(BF₄⁻) • CH₂Cl₂: C, 61.44; H, 4.12; N, 6.03. Found: C, 61.93; H, 4.21; N, 6.03.

2.2.6. Complex 3H

In a Schlenk tube, under Ar atmosphere, DPEPhos (58.4 mg, 0.108 mmol) and Cu(CH₃CN)₄ BF₄ (34.4 mg, 0.11 mmol) were dissolved in 10 ml of dry and freshly distilled CH₂Cl₂. The reagents stirred for an hour at room temperature, before the ligand L3 (21.3 mg, 0.054 mmol) was added (a small amount of CH₃CN was added to increase the solubility of the ligand). After 4 h, the solvent was evaporated by reduced pressure. The residue was dissolved in a

minimum amount of CH₂Cl₂ and recrystallized by slow diffusion of C₆H₁₂. The obtained yellowish-white crystals were filtrated and dried under vacuum. Yield: 76.3 mg, (79.7%). ¹H NMR (500 MHz, 298 K, CDCl₃) δ: 14.41 (broad s, 2H, NH), 7.66 (s, broad, 10H); 7.28 (q, *J* = 9.6, 7.5 Hz, 2H); 7.26 (CHCl₃); 7.13 (s, broad, 10H), 7.01–6.93 (m, 8H), 6.85 (m, 7H), 6.71 (m, 4H), 2.02 (s, 6H). ¹³C NMR (126 MHz, 298 K, CDCl₃) δ: 158.47; 134.61; 132.19; 130.19; 128.78; 128.57; 124.75; 120.23; 99.99; 78.24–77.94 (CDCl₃); 26.94; 25.22. ³¹P NMR (400 MHz, 298 K, CDCl₃) δ: –13.99. HRMS (ESI): 1685.35 (*z* = 1) (C₉₄H₇₄Cu₂N₈O₂P₄BF₄)⁺; 1596.34 (*z* = 2) (C₉₄H₇₄Cu₂N₈O₂P₄H)²⁺. Calcd for C₉₄H₇₄Cu₂N₈O₂P₄H²⁺ 2(BF₄⁻) • CH₂Cl₂: C, 61.44; H, 4.12; N, 6.03. Found: C, 61.73; H, 4.09; N, 6.20.

2.3. Photophysical data

UV–vis absorption spectra were recorded with a Perkin Elmer Lambda 750 double-beam UV/Vis-NIR spectrometer equipped with a 6 × 6 cell changer unit at 20 °C. Luminescence at room temperature was measured using a Jobin–Yvon Fluoromax 4 fluorimeter with a step width of 1 nm and an integration time of 0.8 s. All measurements were performed in pressure resistant quartz cuvettes with septum from Hellma. CH₂Cl₂ solvent for spectroscopic measurements was supplied by Merck (Uvasol). Photoluminescence quantum yields were determined utilizing as reference one of the following standards, depending on the excitation and emission wavelengths: Ru (bpy)₃Cl₂ (6 H₂O) in water; *p*-terphenyl in cyclohexane. Lifetime measurements were performed by time-correlated single-photon counting (TCSPC) with a DeltaTime kit for DeltaDiode source on FluoroMax systems, includes DeltaHub and DeltaDiode controller. The light-source was a NanoLED 366 nm. For time-resolved photoluminescence spectroscopy at 77 K, an actively Q-switched diode pumped solid-state laser (AOT-YVO-20QSP, Advanced Optical Technology Ltd.) with pulse duration of about 1 ns was used. All samples were excited at a wavelength of 355 nm and with an excitation power of 60 μW. The photoluminescence was fibre-coupled into a spectrometer (Acton SpectraPro SP-2300, Princeton Instruments) and detected in a time-dependent manner by a gated CCD-camera (PI-MAX4, Princeton Instruments). Measurements at 77 K were performed by placing cuvettes with the solutions into a liquid nitrogen bath.

2.4. Electrochemical measurements

Cyclic voltammetry experiments were performed with a Metrohm Autolab PGSTAT101 inside a glovebox. The electrochemical cell was equipped with a Pt-disc as working electrode, an Ag-wire quasi-reference electrode and a Pt wire as counter electrode. Ferrocene was used as internal standard. All the redox potentials are reported versus the standard calomel electrode (SCE). The electrochemical characterization, cyclic voltammetry (CV), was performed in solutions of 0.1 M tetrabutylammonium hexafluorophosphate (TBAPF₆). Electrochemical solvents used are dry acetonitrile (ACN) and *N,N*-dimethylformamide (DMF). The concentration of the samples was in the millimolar range: 2.8 mM (**1H**); 1.6 mM (**2H**); 1.1 mM (**3H**); 17.9 mM (**L1**); 6.3 mM (**L2**); 9.5 mM (**L3**); 14.1 mM ([Ni(cyclam)Cl₂]). TBAPF₆ (electrochemical grade, 99%, Fluka) was used as the supporting electrolyte, which was recrystallized from an ethanol solution and dried at 60 °C under vacuum.

2.5. Computational details

All quantum chemical calculations were performed with the Turbomole 7.2.1 package [43]. Models for the Ligands **L1–L3** and the complexes **1H–3H** were fully relaxed at the DFT BP86-D3 level

(neglecting the BF_4^- anion in the calculations) with a mixed basis set based on the def2-family [44,45]. The Cu ion and the coordinating P and N atoms were described by a def2-TZVP basis, the rest of the molecule by a def2-SVP basis set. Dispersion interactions in all simulations were considered with the Grimme -D3 approach [46] including a damping function as introduced by Becke and Johnson (BJ) [47]. Solvent effects were modelled with an implicit solvent model (COSMO) [48] utilizing a value of $\epsilon = 8.93$ for the dielectric constant of dichloromethane. A fine grid (size 4) was used in all numerical integrations using strict convergence criteria for the energy ($<10^{-7}$ H) and density ($<10^{-7}$). Structural relaxations were considered converged if the maximum norm of the Cartesian gradient had dropped below 10^{-4} H/Bohr. The ten lowest electronically excited states (singlets) were calculated for all models in solution within the linear response formalism of the adiabatic time-dependent density functional theory (TDDFT) employing the hybrid BH-LYP functional (to take care of charge transfer excitations) and the same basis as in the relaxations of the structural parameters.

3. Results and discussion

3.1. Synthesis of ligands and synthesis of complexes

The ligands were prepared in two steps. First, 6-bromo-2-methylpyridine reacted with the triple bond of an ethynyl-derivative via a Sonogashira cross-coupling reaction. The second step was a 1,3-Huisgen reaction between the so-formed alkyne and a trimethylsilylazide at high temperature. The obtained 1*H*-1,2,3-triazoles were substituted in the 4 and 5 positions, with a phenyl and a pyrid-2-yl ring, respectively (Scheme 1). In order to obtain dinuclear complexes with metal centres that are electronically coupled, we chose a phenyl ring to be the bridging unit.

The synthesis of the final copper complexes was conducted in inert atmosphere, as it is well known that Cu(I) is easily oxidised to Cu(II), especially in aerated solutions. The solvent used for the reaction was dry and freshly distilled dichloromethane (DCM). The coordination of the diphosphine ligand DPEPhos with the metal centre occurred at first by reaction with the tetrakis (acetonitrile) copper tetrafluoroborate. At a later time, the appropriate equivalents of the chelating N N ligand were added. The final complexes were salts. In fact, no deprotonation of the triazole ring occurred; therefore, the ligand stayed neutral, and upon coordination with the positively charged metal core, the BF_4^- counteranion was present in order to maintain electroneutrality. In Scheme 2 the synthesis of the heteroleptic mononuclear Cu(I) complex **1H** is shown, together with the chemical structures of complexes **2H** and **3H**. The

complexes were purified by recrystallization in cyclohexane. The yield after purification of these complexes was close to 80%.

3.2. X-ray structure of complex 1H

Crystallisation by slow diffusion of cyclohexane into a concentrated DCM solution of **1H** provided colourless crystals, suitable for X-ray analysis. The solved molecular structure is shown in Fig. 1, and selected parameters of the molecular structure are given in Table 1. The geometric parameters are comparable with the distances and angles reported for other mononuclear heteroleptic Cu(I) complexes [49,50].

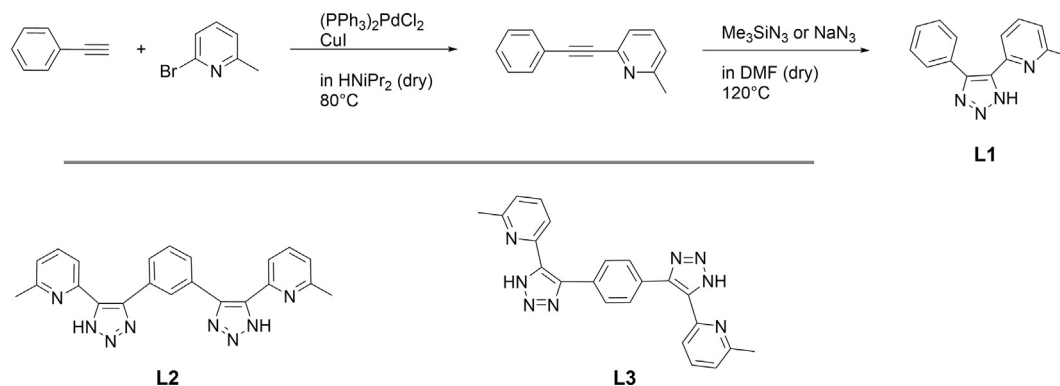
Quantum chemical calculations at the density functional theory (DFT) level gave a structure in good agreement to the experimental one (see Table S2 and Fig. S12 in ESI). However, compared to the experimental obtained structure **1H** the two N-Cu-P bond angles are more symmetric. Inclusion of the solvent CH_2Cl_2 by the conductor like screening model (COSMO) did not change the atomic positions significantly.

3.3. Spectroscopic properties

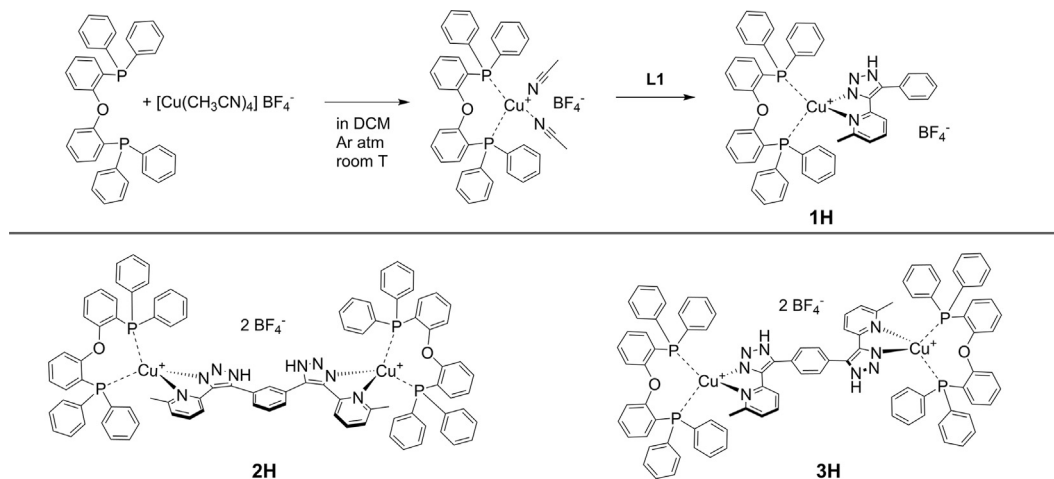
3.3.1. Electronic absorption

The photophysical properties of the three heteroleptic Cu(I) complexes were investigated at room temperature in dichloromethane as spectroscopic solvent. The absorption profiles of the complexes were quite similar to each other and their absorptivity coefficients are shown in Fig. 2. All three complexes show an intense absorption around 270 nm, which can be attributed to $\pi-\pi^*$ transitions, localised on the chelating phosphine and on the N N ligand. In fact, in the high energy region, the electronic transitions are dominated by $\pi-\pi^*$ and by $n-\pi^*$ intra-ligand transitions. The absorptivity coefficients of the new ligands in dichloromethane are shown in Fig. 2 (dashed lines) and in the supporting information (Fig. S2). The difference in intensity between the dinuclear complexes and the mononuclear one, the concentrations being equal, is due to the fact that the dimers contain two DPEPhos units. The shoulders with highest absorption peak close to 300 nm are related to the intra-ligand transitions occurring on the ligands. The lower-energy absorptions are due to the electronic transitions from the d-orbitals of the Cu(I) metal centre to the π^* of the pyridyl-triazole ligand, involving the population of the singlet MLCT state. These results are supported by TDDFT calculations for **1H** (for details see ESI: Quantum chemical calculations sections). In Fig. S12, the MLCT character of the lowest excited state is shown.

The increase of the absorptivity coefficient of the dinuclear



Scheme 1. Synthesis of the monochelate 4-phenyl-5-(6'-methyl-pyrid-2'-yl)-1*H*-1,2,3-triazole **L1** in two steps. The chemical structures of the bis-bidentate ligands **L2** and **L3** are also shown.



Scheme 2. Synthesis of the heteroleptic Cu(I) complex **1H** in dry and freshly distilled DCM. In the same manner the complexes **2H** and **3H** (bottom) were prepared, after addition of 0.5 equivalents of ligands **L2** and **L3**, respectively.

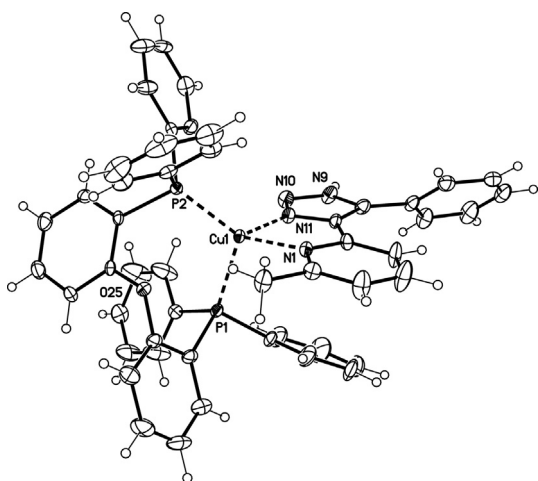


Fig. 1. Molecular structure of **1H**. (BF_4 anion and solvent are omitted for clarity; displacement parameters are drawn at 50% probability level).

compounds **2H** and **3H** in comparison to the mononuclear complex **1H** is due to the presence of two coordinated centres. Nevertheless, the increase for the complex **3H** is higher than **2H**, suggesting that an electronic communication between the two coordinated sites should be present in **3H**. For **2H** and **3H**, two transitions with the same excitation energy but different transition dipole moments are the origin of the peak at ca. 300 nm. In **2H**, both transitions have an appreciable intensity, whereas only one excitation contributes significantly in **3H**, where the transition dipole moments of the two halves are almost parallel to each other. Taking both excitations into account, **3H** has a slightly higher intensity than **2H** (see [Fig.s S16, S17 and S18](#)).

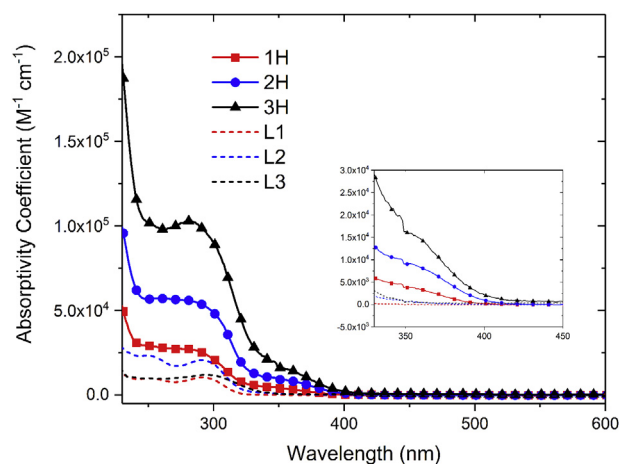


Fig. 2. Absorption spectra in CH_2Cl_2 of the complexes investigated in this work: **1H** (red-squares line); **2H** (blue-circles line) and **3H** (black-triangles line). The absorptivity coefficients of the ligands are reported in dashed lines (**L1**: red; **L2**: blue; **L3**: black). (In the inset, an enlargement of the absorption between 330 and 450 nm is shown). (For interpretation of the references to colour in this figure legend, the reader is referred to the Web version of this article.)

A similar trend can be recognized in the absorptivity coefficients of the ligands **L1** and **L2**; in fact, their absorption spectra are almost identical, but the intensity in **L2** is almost twice the value of **L1**, while ligand **L3** shows a different profile.

3.3.2. Emission in solution at room temperature

Photophysical investigation of the free ligands and of the three complexes was performed in CH_2Cl_2 solutions. The photophysical properties are reported in [Table 2](#) and the emission and excitation

Table 1
Selected bond lengths (Å) and bond angles (deg) for **1H**.

Bond lengths (Å)		Bond angles (deg)	
Cu1-N11	2.038 (4)	N11-Cu1-N1	79.93 (15)
Cu1-N1	2.095 (4)	N11-Cu1-P2	123.20 (12)
Cu1-P2	2.2168 (13)	N1-Cu1-P2	125.78 (12)
Cu1-P1	2.2742 (13)	N11-Cu1-P1	102.51 (13)
		N1-Cu1-P1	104.44 (12)
		P2-Cu1-P1	114.59 (5)

Table 2
Spectroscopic and photophysical properties at room temperature and at 77 K.

Sample	$\lambda_{\text{abs}}^{\text{a,b}}/\text{nm}$ ($\epsilon/M^{-1}\text{ cm}^{-1}$)	$\lambda_{\text{em}}^{\text{a,b}}/\text{nm}$	$\Phi^{\text{a,b,c}}$	$\tau^{\text{a,b}}/\mu\text{s}$	$k_{\text{r}} (\times 10^4)/\text{s}^{-1}$	$k_{\text{nr}} (\times 10^5)/\text{s}^{-1}$	$\lambda_{\text{em}}^{\text{d}}/\text{nm}$ (77 K)	$\tau^{\text{d}}/\mu\text{s}$ (77 K)
L1	250 (9.9×10^3), 292 (10.5×10^3)	352	0.038 ^e	0.007	563	1352		
L2	250 (2.2×10^4), 292 (20.7×10^3)	352	0.020 ^e	0.007	298	1463		
L3	250 (9.9×10^3), 295 (11.9×10^3)	369	0.221 ^e	0.003	6875	2438		
1H	281 (2.74×10^4), 350 (3.85×10^3)	554	0.054	0.88	6.1	10.7	527	200
2H	281 (5.59×10^4), 350 (9.04×10^3)	556	0.099	1.21	8.2	7.4	529	214
3H	281 (1.03×10^5), 350 (1.63×10^4)	556	0.142	2.78	5.1	3.1	527	256

^a In DCM.

^b Ar-saturated solution.

^c Quantum yields were determined with the relative method using Ru (bpy)₃Cl₂ as reference (in aerated water solution $\phi = 0.028$).

^d In a glass matrix of EtOH/MeOH (4:1); emission decays were analysed with monoexponential fit.

^e in aerated DCM solution using *p*-terphenyl as reference (in aerated cyclohexane solution $\phi = 0.92$).

spectra of the free ligands and of the Cu(I) complexes are shown in Fig. 3 and in Fig. 4, respectively. Luminescence of the free ligands can be described as fluorescence with maximum energy at 352 nm for **L1** and **L2**, while **L3** emits at lower energy (maximum at 369 nm), clearly due to the extended conjugation of the system. Photoluminescence quantum yield of ligand **L3** is 22.1%, a much higher value than **L1** (3.8%) and **L2** (2.0%). Lifetimes of their excited state are in the range of nanoseconds. The three investigated complexes are strongly luminescent and exhibit unstructured broad emission with large Stokes shifts (Fig. 4). These features point to an emissive excited state with a dominant metal-to-ligand charge-transfer character. The emission maxima were 554 nm for complex **1H**, and 556 nm for complexes **2H** and **3H**. The excitation spectra were recorded by monitoring the emission maximum of the corresponding complex. Their profiles are very similar to each other, and recall the observed absorption spectra. The emission quantum yields measured in Ar-saturated atmosphere are reasonably high for Cu(I) complexes. The mononuclear Cu(I) complex **1H** has a photoluminescence quantum yield Φ of 5.4%, which is a good result with regard to other mononuclear heteroleptic complexes of similar structure (Fig. 5) [49–51]. The increased emission might be due to the steric hindrance caused by the presence of the methyl group *alpha* to the N of the pyridine. The structural rigidity, in fact,

leads to a lower reorganisation of the ligands around the excited Cu(I) core. This is evident comparing the photophysical properties of **1H** with the neutral complex **C** in Fig. 5. Complex **C** has an unsubstituted pyrid-2'-yl-1*H*-1,2,3-triazole as N,N chelating ligand. The absence of any sterical hindrance in this ligand allows a great flattening distortion in the excited state, diminishing the photoluminescence quantum yield ($\Phi = 0.6\%$ for **C**) [50]. Compounds **A** and **B** have 1*H*-1,2,4-triazoles instead of 1*H*-1,2,3-triazole and, although these N,N ligands do not have any substituents in *alpha* to the N atom of the pyridine, they have substituents in the triazole ring. Neutral complex **A** has comparable photophysical properties in respect to **1H**, with almost identical emission energy (555 nm for **A**) and quantum yield (5.0% for **A**) [49]. In the charged Cu(I) complex **B**, the triazole coordinates the metal core with the N atom in position 4, which is less common for this kind of triazole. The presence of a *t*-butyl substituent in position 5 enhances the rigidity in the excited state, affording higher quantum yield (14.0%) and long-lived excited state lifetime (15.0 μs) [51]. Interestingly, the dinuclear complexes showed much stronger emission than the mononuclear complex **1H**. The dinuclear complex **2H** features two coordinating units bridged in the *meta* position and has a Φ of 9.9%, whereas complex **3H**, with a *para*-substituted bridging ligand,

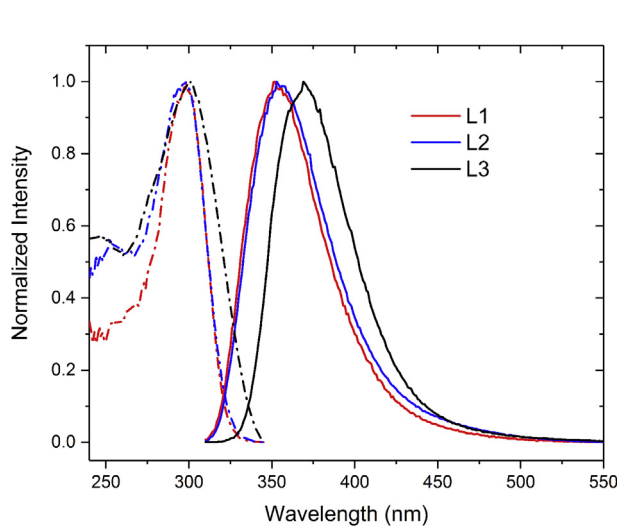


Fig. 3. Excitation (dashed-dotted) and emission (solid) spectra of free ligands **L1** (red line), **L2** (blue line) and **L3** (black line) in air-equilibrated CH₂Cl₂ solution. ($\lambda_{\text{exc}} = 295\text{ nm}$). (For interpretation of the references to colour in this figure legend, the reader is referred to the Web version of this article.)

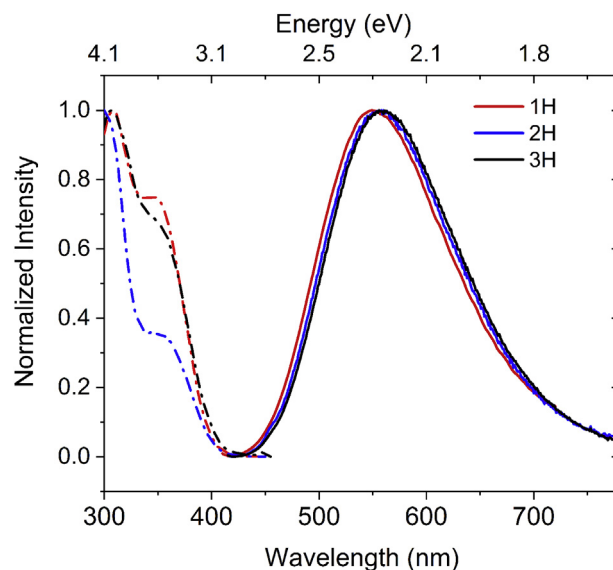


Fig. 4. Excitation (dashed-dotted) and emission (solid) spectra of complexes **1H**, **2H** and **3H** in Ar-saturated CH₂Cl₂ solution. ($\lambda_{\text{exc}} = 365\text{ nm}$).

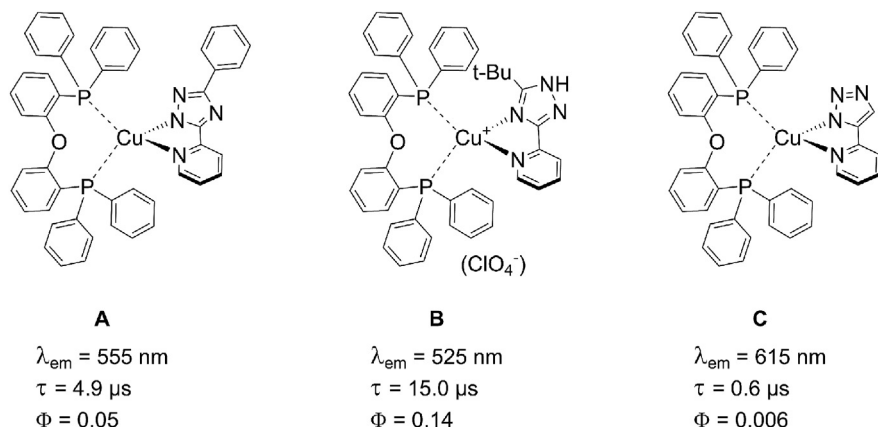


Fig. 5. Selected heteroleptic Cu(I) complexes, **A** [49], **B** [51], **C** [50], with N,N chelating ligands that are analogue to **L1**, investigated in this work. The reported photophysical properties were measured in CH_2Cl_2 at room temperature.

showed a Φ of 14.2%. Along with the increasing emission quantum yield, the excited state lifetimes also increased. Mononuclear complex **1H** has an excited state lifetime τ of 0.88 μ s, and dinuclear complexes **2H** and **3H** have lifetimes of 1.21 μ s and 2.78 μ s, respectively. The phenomenon of significant increase of quantum yields and lifetimes for dinuclear Cu(I) complexes compared to the mononuclear one reflects the influence of the second metal centre on the photophysical properties of these complexes, especially in **3H**. The fully π -conjugated system seems to mediate a strong electronic communication between the metal cores, as already indicated for the absorption spectra. Possible cooperative effects between the metal centres are currently under investigation.

Emission in a glassy matrix at 77 K. Photoluminescence and lifetime of the three complexes were also measured in frozen matrices of ethanol/methanol (4:1). We measured the low-temperature photoluminescence also in a glassy matrix of dichloromethane, (Fig. S6 and Table S1). Since the broad emission structure persists also at low temperature, the MLCT state is the emissive state even at 77 K, with no contribution from ligand-centred transitions (Fig. 6). Moreover, for all three compounds there is a hypsochromic shift (ca. 0.07 cm^{-1}), due to a rigidochromic effect. This shift to higher energy is more pronounced when the

frozen matrix is dichloromethane (ca. 0.12 cm^{-1}). From the observations above, we can conclude that the more rigid environment of the frozen matrix allows the emission from a $^3\text{MLCT}$ state that is not stabilised by solvent rearrangement, as it happens at room temperature. The long decay lifetimes are in the range of 200 μ s, in agreement with other Cu(I) complexes [49,52,53].

This is supported by quantum chemical calculations. The Cu coordination of the lowest triplet excited state is shown in Tables S2 and S3 and Fig. S12, where also the different density between ground and excited state is shown, which supports the MLCT character. The local structure at the Cu centre is only slightly distorted. It is not as symmetric as in the ground state calculation. The N-Cu-P angles are similar to the experimental values. The calculated Stokes shift amounts to 2.12 eV.

3.4. Electrochemical properties

The three complexes were characterised also by cyclic voltammetry, in order to investigate their electrochemical behaviour. The working and counter electrodes were a platinum disk and a platinum wire, respectively. Since a silver wire was used as the pseudoreference electrode, ferrocene as internal standard was necessary [54]. The solvent was dry acetonitrile, with 0.1 M concentration of the supporting electrolyte, tetrabutylammonium hexafluorophosphate (TBAPF₆). The redox processes are not reversible. The oxidation is expected to occur primarily on the copper metal site ($E_{1/2} = 1.70$ V, 1.75 V and 1.79 V versus standard calomel electrode (SCE) for **1H**, **2H** and **3H** respectively); a second oxidation process is mainly localised on the chelating diphosphine ligand. On the other hand, the reduction process should be concentrated on the N,N chelating ligands ($E_{1/2}$ around -2.35 V versus SCE for all three complexes **1H**, **2H** and **3H**). Cyclic voltammetry of the free ligands was recorded in N,N-dimethylformamide (DMF), in order to have a wider solvent window in the reduction process. The ligands present irreversible reduction ($E_{1/2} = -2.11$ V (**L1**); -2.21 (**L2**); -2.05 (**L3**) vs SCE) (see Fig. S7 and S8). The redox processes of **1H** were investigated at different scan rates (see Fig. S9). The irreversibility of the oxidation is retained, while the reduction becomes quasi-reversible at a scan rate of 500 mV/s. As expected from the photophysical studies, the difference in energy between the first oxidation and the first reduction is very similar in all three complexes. (See Table 3 and Fig. 7 for details). The frontier orbitals HOMO and LUMO are indirectly related to the oxidation and reduction potentials, thus we estimated their values using empirical relations, utilizing the oxidation and reduction potentials

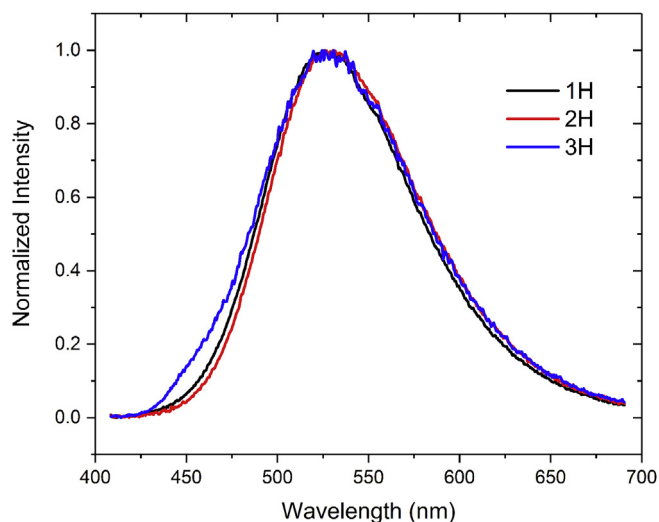


Fig. 6. Emission spectra of complexes **1H**, **2H** and **3H** in a frozen matrix of EtOH/MeOH (4:1) at 77 K.

Table 3
Electrochemical data of complexes in acetonitrile (0.1 M TBAPF₆) at room temperature.^a

Sample	E _{ox} /V	E _{red} /V	HOMO ^b /eV	LUMO ^c /eV	Δ _{HOMO-LUMO} /eV
1H	1.30	−2.35	−6.10	−2.05	4.05
2H	1.35	−2.33	−6.15	−2.07	4.08
3H	1.39	−2.35	−6.19	−2.05	4.14
L1		−2.04 ^d		−2.29	
L2		−2.14 ^d		−2.19	
L3		−1.98 ^d		−2.35	

^a Values obtained by cyclic voltammetry, scan rate 100 mV/s, reported versus the standard calomel electrode (SCE).

^b Estimated from oxidation potential versus ferrocene/ferrocenium potential.

^c Estimated from reduction potential versus ferrocene/ferrocenium potential.

^d In dry DMF (0.1 M TBAPF₆).

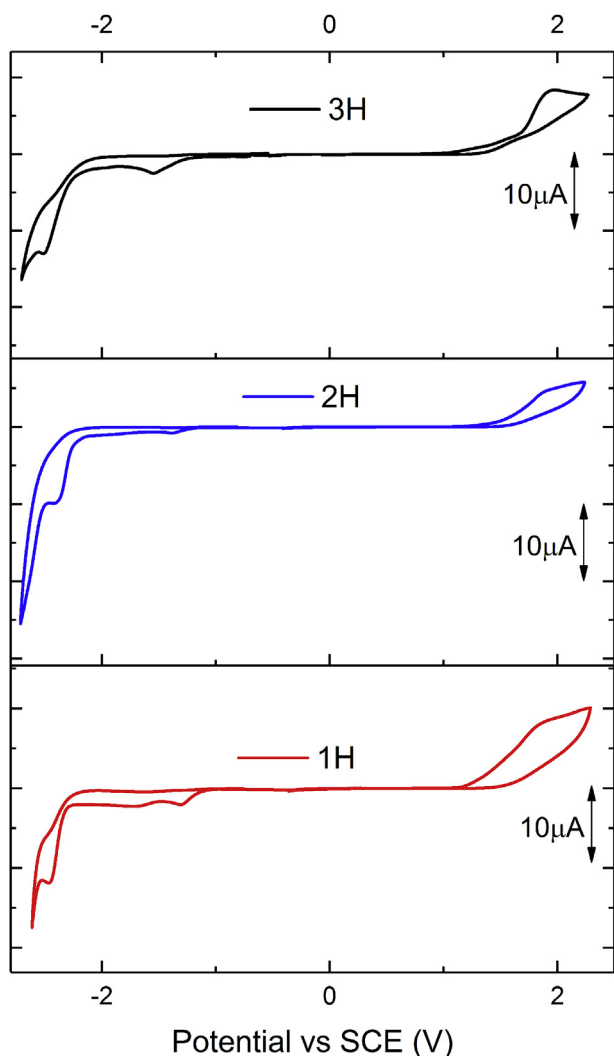


Fig. 7. Cyclic voltammetry of complexes **1H**, **2H** and **3H** in acetonitrile (0.1 M TBAPF₆) at a scan rate of 100 mV/s.

of the complexes in respect to the oxidation potential of the ferrocene [55].

In order to use **1H**, **2H**, and **3H** as photosensitizers (PS) it is of utmost importance to determine the excited state redox processes E_{ox}(PS*) and E_{red}(PS*) (respectively the oxidation and the reduction potentials of the PS in its excited state). Therefore, we

Table 4
Estimation of the excited state processes in ACN at room temperature versus Fc/Fc⁺.

Sample	E ₀₋₀ /V	E _{ox} (PS*)/V	E _{red} (PS*)/V
1H	3.23	−1.93	0.48
2H	3.20	−1.85	0.47
3H	3.22	−1.83	0.47

estimated the energy of the excited state E₀₋₀ in acetonitrile for each complex. Details are available in the supporting information. The excited-state redox processes are reported versus Fc/Fc⁺ in Table 4.

These values are used to evaluate if a photoinduced electron transfer process (reductive or oxidative quenching) is energetically feasible (*vide infra*).

3.5. Stern–Volmer bimolecular quenching

Our target is to develop new photosensitizers (PS) that can be used in the photoactivation of small molecules. The heteroleptic complexes that we have presented here have a long-lived excited state, which is an important characteristic for a PS. Hereafter we report a preliminary experiment of Stern–Volmer bimolecular quenching of the three complexes with the catalyst Ni(cyclam)Cl₂. In fact, Ni(cyclam)Cl₂ was used in both electrochemical and photochemical reduction of CO₂ to CO, showing high stability and selectivity for CO₂ over H₂O [42,56]. These experiments were conducted in aerated acetonitrile solution (τ_{aer} = 54 ns (**1H**); 57 ns (**2H**); 195 ns (**3H**)). A solution of Ni(cyclam)Cl₂ (1 × 10^{−3} M) in ACN was prepared and added in 50 μL steps to the PS solution in order to identify a possible quenching. Fig. 8 shows the ratio of the emission intensity (I₀/I) as a function of the concentration of Ni(cyclam)Cl₂ ([CAT]). It reveals that the emission of the three complexes suffers from the increasing presence of the Ni catalyst. The Stern–Volmer equation was used in order to fit the data in Fig. 8. The Stern–Volmer constants are: 1.90 mM^{−1} (**1H**); 1.16 mM^{−1} (**2H**) and 3.27 mM^{−1} (**3H**), from which we can estimate the apparent quenching rate constant to be 3.5 × 10¹⁰ s^{−1} M^{−1} (**1H**); 2.0 × 10¹⁰ s^{−1} M^{−1} (**2H**); 1.7 × 10¹⁰ s^{−1} M^{−1} (**3H**). At this stage we can observe that all three Cu(I) complexes are quenched by the presence of the catalyst, which is a requirement in order to use the

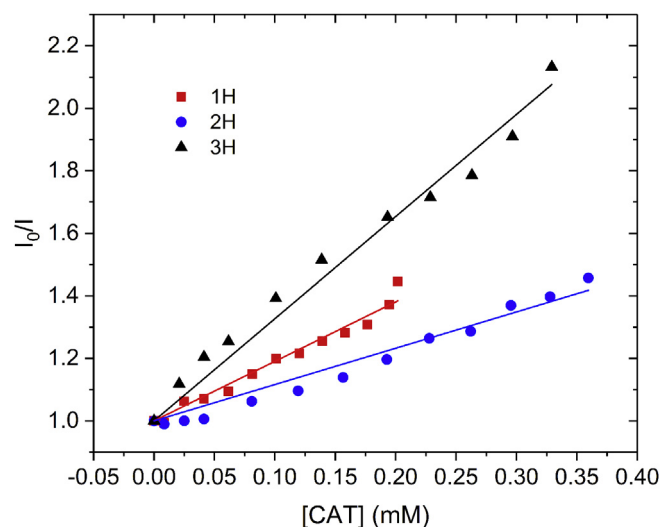


Fig. 8. Plot of the ratio of the intensities (calculated at emission maximum) I₀/I of the three complexes versus the concentration of the Ni(cyclam)Cl₂ (CAT) in ACN. The absorbance at the excitation wavelength was constant after each measurement.

system Cu(I) complex **3H** and Ni(cyclam)Cl₂ as PS and CAT for the photoreduction of CO₂. This is also in accordance with the fact that Cu(I) complexes undergo oxidative, rather than reductive, quenching [23]. An estimation of the driving force for the oxidative quenching can be calculated by the following equation: $\Delta G = E_{ox}(PS^*) - E_{red}(CAT)$. In this case, CAT is Ni(cyclam)Cl₂ (E_{red} in ACN = 1.73 V versus Fc/Fc⁺). Thus, the oxidative quenching of the excited state by Ni(cyclam)Cl₂ results energetically feasible for the investigated complexes ($\Delta G(\mathbf{1H}) = -0.20$; $\Delta G(\mathbf{2H}) = -0.12$; $\Delta G(\mathbf{3H}) = -0.10$).

4. Conclusion

We have presented one mononuclear and two dinuclear heteroleptic copper(I) complexes based on pyrid-2'-yl-1H-1,2,3-triazole as N,N chelating ligand and DPEPhos as chelating diphosphine. The presence of the methyl group *alpha* to N of the pyridyl ring increases the structural rigidity, leading to a lower structural reorganisation in the excited state. Thus, these complexes possess good luminescence properties in solution at room temperature. The hypsochromic shift in frozen matrix at 77 K is due to a rigidochromic effect. The excited-state lifetime of the dinuclear complex **3H** is much longer than for the mononuclear compound, which we postulate is due to electronic interaction between both metal centres in the binuclear complexes. The excited-state redox processes of the three complexes were evaluated and bimolecular quenching experiments with Ni(cyclam)Cl₂ were performed, in order to prove the photoinduced redox process, which is needed for their application in the photoreduction of CO₂. This promising application is the subject of investigation in our laboratory.

Notes

The authors declare no conflict of interest.

Acknowledgement

We gratefully acknowledge funding support from the DFG-funded Collaborative Research Centres (SFB) TRR 88/3MET "Cooperative Effects in Homo- and Heterometallic Complexes" (CB: overhead of 3MET package (B2); KF, SK: project B1). CB thanks Prof. S. Bräse (KIT) for his scientific support. We thank Prof. F. Breher (KIT), Prof. H.-A. Wagenknecht (KIT) and Prof. U. Lemmer (KIT) for giving access to electrochemical and photochemical equipment, respectively. Dr. P. Weis is acknowledged for high-resolution mass spectrometry measurements.

Appendix A. Supplementary data

Computational details. CCDC 1810640 (**1H**). For ESI and crystallographic data in CIF or other electronic format.

Supplementary data related to this article can be found at <https://doi.org/10.1016/j.jorganchem.2018.07.013>.

References

- [1] P. Anastas, N. Eghbali, *Green chemistry: principles and practice*, Chem. Soc. Rev. 39 (1) (2010) 301–312.
- [2] J. Zhao, W. Wu, J. Sun, S. Guo, Triplet photosensitizers: from molecular design to applications, Chem. Soc. Rev. 42 (12) (2013) 5323–5351.
- [3] N. Zivic, M. Bouzrati-Zerelli, A. Kermagoret, F. Dumur, J.-P. Fouassier, D. Gimes, J. Lalevée, Photocatalysts in polymerization reactions, ChemCatChem 8 (9) (2016) 1617–1631.
- [4] C.K. Prier, D.A. Rankic, D.W.C. MacMillan, Visible light photoredox catalysis with transition metal complexes: applications in organic synthesis, Chem. Rev. 113 (7) (2013) 5322–5363.
- [5] N. Corrigan, S. Shanmugam, J. Xu, C. Boyer, Photocatalysis in organic and polymer synthesis, Chem. Soc. Rev. 45 (22) (2016) 6165–6212.
- [6] D.M. Schultz, T.P. Yoon, Solar synthesis: prospects in visible light photocatalysis, Science 343 (6174) (2014) 1239176.
- [7] M. Grätzel, Solar energy conversion by dye-sensitized photovoltaic cells, Inorg. Chem. 44 (20) (2005) 6841–6851.
- [8] K. Willinger, M. Thelakkat, Photosensitizers in solar energy conversion, in: T. Nyokong, V. Ahseen (Eds.), Photosensitizers in Medicine, Environment, and Security, Springer Netherlands, Dordrecht, 2012, pp. 527–617.
- [9] B. Bozic-Weber, E.C. Constable, C.E. Housecroft, Light harvesting with Earth abundant d-block metals: development of sensitizers in dye-sensitized solar cells (DSCs), Coord. Chem. Rev. 257 (21) (2013) 3089–3106.
- [10] C.B. Larsen, O.S. Wenger, Photoredox catalysis with metal complexes made from earth-abundant elements, Chem. Eur. J. 24 (2018) 2039–2058.
- [11] Y. Zhang, M. Schulz, M. Wächter, M. Karnahl, B. Dietzek, Heteroleptic diimine–diphosphine Cu(I) complexes as an alternative towards noble-metal based photosensitizers: design strategies, photophysical properties and perspective applications, Coord. Chem. Rev. 356 (2018) 127–146.
- [12] O. Horváth, Photochemistry of copper(I) complexes, Coord. Chem. Rev. 135–136 (Supplement C) (1994) 303–324.
- [13] N. Armaroli, G. Accorsi, F. Cardinalli, A. Listorti, Photochemistry and photophysics of coordination compounds: copper, in: V. Balzani, S. Campagna (Eds.), Photochemistry and Photophysics of Coordination Compounds I, Springer Berlin Heidelberg, Berlin, Heidelberg, 2007, pp. 69–115.
- [14] A. Kaeser, M. Mohankumar, J. Mohanraj, F. Monti, M. Holler, J.J. Cid, O. Moudam, I. Nierengarten, L. Karmazin-Brelot, C. Duhayon, B. Delavaux-Nicot, N. Armaroli, J.F. Nierengarten, Heteroleptic copper(I) complexes prepared from phenanthroline and bis-phosphine ligands, Inorg. Chem. 52 (20) (2013) 12140–12151.
- [15] F. Dumur, Recent advances in organic light-emitting devices comprising copper complexes: a realistic approach for low-cost and highly emissive devices? Org. Electron. 21 (Supplement C) (2015) 27–39.
- [16] E. Fresta, R.D. Costa, Beyond traditional light-emitting electrochemical cells - a review of new device designs and emitters, J. Mater. Chem. C 5 (23) (2017) 5643–5675.
- [17] C. Bizzarri, E. Spuling, D.M. Knoll, D. Volz, S. Bräse, Sustainable metal complexes for organic light-emitting diodes (OLEDs), Coord. Chem. Rev. (2017). <https://doi.org/10.1016/j.ccr.2017.09.011>.
- [18] R.D. Costa, D. Tordera, E. Orti, H.J. Bolink, J. Schonke, S. Graber, C.E. Housecroft, E.C. Constable, J.A. Zampese, Copper(I) complexes for sustainable light-emitting electrochemical cells, J. Mater. Chem. 21 (40) (2011) 16108–16118.
- [19] *dap* is 2,9-bis(para-anisyl)-1,10-phenanthroline.
- [20] J.-M. Kern, J.-P. Sauvage, Photoassisted C-C coupling via electron transfer to benzylic halides by a bis(di-imine) copper(I) complex, J. Chem. Soc., Chem. Commun. 8 (1987) 546–548.
- [21] D. Li, C.-M. Che, H.-L. Kwong, V.W.-W. Yam, Photoinduced C-C bond formation from alkyl halides catalysed by luminescent dinuclear gold(I) and copper(I) complexes, J. Chem. Soc., Dalton Trans. 23 (1992) 3325–3329.
- [22] O. Reiser, Shining light on copper: unique opportunities for visible-light-catalyzed atom transfer radical addition reactions and related processes, Acc. Chem. Res. 49 (9) (2016) 1990–1996.
- [23] S. Paria, O. Reiser, Copper in photocatalysis, ChemCatChem 6 (9) (2014) 2477–2483.
- [24] A.C. Hernandez-Perez, S.K. Collins, Heteroleptic Cu-Based sensitizers in photoredox catalysis, Accounts Chem. Res. 49 (8) (2016) 1557–1565.
- [25] M.S. Lazorski, F.N. Castellano, Advances in the light conversion properties of Cu(I)-based photosensitizers, Polyhedron 82 (Supplement C) (2014) 57–70.
- [26] M. Pirtsch, S. Paria, T. Matsuno, H. Isobe, O. Reiser, [Cu(dap)2Cl] as an efficient visible-light-driven photoredox catalyst in carbon–carbon bond-forming reactions, Chem. Eur. J. 18 (24) (2012) 7336–7340.
- [27] M. Majek, A. Jacobi von Wangelin, Ambient-light-mediated copper-catalyzed C-C and C-N bond formation, Angew. Chem. Int. Ed. 52 (23) (2013) 5919–5921.
- [28] M.M. Cetin, R.T. Hodson, C.R. Hart, D.B. Cordes, M. Findlater, D.J. Casadonte Jr., A.F. Cozzolino, M.F. Mayer, Characterization and photocatalytic behavior of 2,9-di(aryl)-1,10-phenanthroline copper(I) complexes, Dalton Trans. 46 (20) (2017) 6553–6569.
- [29] T.P. Nicholls, G.E. Constable, J.C. Robertson, M.G. Gardiner, A.C. Bissember, Brønsted acid cocatalysis in copper(I)-photocatalyzed α -amino C–H bond functionalization, ACS Catal. 6 (1) (2016) 451–457.
- [30] M. Knorn, T. Rawner, R. Czerwieńiec, O. Reiser, [Copper(phenanthroline)(bisisonitrile)]⁺-Complexes for the visible-light-mediated atom transfer radical addition and allylation reactions, ACS Catal. 5 (9) (2015) 5186–5193.
- [31] G. Fumagalli, P.T.G. Rabet, S. Boyd, M.F. Greaney, Three-component azidation of styrene-type double bonds: light-switchable behavior of a copper photoredox catalyst, Angew. Chem. 127 (39) (2015) 11643–11646.
- [32] D.B. Bagal, G. Kachkovskiy, M. Knorn, T. Rawner, B.M. Bhanage, O. Reiser, Trifluormethylchlorosulfonylierung von Alkenen – hinweise auf einen Innensphärenmechanismus eines Kupferphenanthrolin-Photoredoxkatalysators, Angew. Chem. 127 (24) (2015) 7105–7108.
- [33] S. Berardi, S. Drouet, L. Francas, C. Gimbert-Surinach, M. Guttentag, C. Richmond, T. Stoll, A. Llobet, Molecular artificial photosynthesis, Chem. Soc. Rev. 43 (22) (2014) 7501–7519.
- [34] D. Gust, T.A. Moore, A.L. Moore, Solar fuels via artificial photosynthesis, Accounts Chem. Res. 42 (12) (2009) 1890–1898.
- [35] A. Rosas-Hernández, C. Steinlechner, H. Junge, M. Beller, Earth-abundant

- photocatalytic systems for the visible-light-driven reduction of CO₂ to CO, *Green Chem.* 19 (10) (2017) 2356–2360.
- [36] S. Fischer, D. Hollmann, S. Tschierlei, M. Karnahl, N. Rockstroh, E. Barsch, P. Schwarzbach, S.-P. Luo, H. Junge, M. Beller, S. Lochbrunner, R. Ludwig, A. Brückner, Death and rebirth: photocatalytic hydrogen production by a self-organizing copper–iron system, *ACS Catal.* 4 (6) (2014) 1845–1849.
- [37] M. Karnahl, E. Mejía, N. Rockstroh, S. Tschierlei, S.-P. Luo, K. Grabow, A. Kruth, V. Brüser, H. Junge, S. Lochbrunner, M. Beller, Photocatalytic hydrogen production with copper photosensitizer–titanium dioxide composites, *ChemCatChem* 6 (1) (2014) 82–86.
- [38] E. Mejía, S.-P. Luo, M. Karnahl, A. Friedrich, S. Tschierlei, A.-E. Surkus, H. Junge, S. Gladiali, S. Lochbrunner, M. Beller, A noble-metal-free system for photocatalytic hydrogen production from water, *Chem. Eur. J.* 19 (47) (2013) 15972–15978.
- [39] H. Takeda, K. Ohashi, A. Sekine, O. Ishitani, Photocatalytic CO₂ reduction using Cu(I) photosensitizers with a Fe(II) catalyst, *J. Am. Chem. Soc.* 138 (13) (2016) 4354–4357.
- [40] J. Windisch, M. Oraziotti, P. Hamm, R. Alberto, B. Probst, General scheme for oxidative quenching of a copper bis-phenanthroline photosensitizer for light-driven hydrogen production, *ChemSusChem* 9 (13) (2016) 1719–1726.
- [41] **Cyclam Is 1,4,8,11-tetraazacyclotetradecane.**
- [42] E. Kimura, X. Bu, M. Shionoya, S. Wada, S. Maruyama, A new Nickel(II) cyclam (cyclam = 1,4,8,11-tetraazacyclotetradecane) complex covalently attached to Ru(phen)₃³⁺ (phen = 1,10-phenanthroline). A new candidate for the catalytic photoreduction of carbon dioxide, *Inorg. Chem.* 31 (1992) 4542–4546.
- [43] **TURBOMOLE V6.2 2010**, A Development of University of Karlsruhe and Forschungszentrum Karlsruhe GmbH, 1989–2007, TURBOMOLE GmbH, since 2007 available from: <http://www.turbomole.com/>.
- [44] A. Schäfer, H. Horn, R. Ahlrichs, Fully optimized contracted Gaussian basis sets for atoms Li to Kr, *J. Chem. Phys.* 97 (4) (1992) 2571–2577.
- [45] A. Schäfer, C. Huber, R. Ahlrichs, Fully optimized contracted Gaussian basis sets of triple zeta valence quality for atoms Li to Kr, *J. Chem. Phys.* 100 (8) (1994) 5829–5835.
- [46] S. Grimme, J. Antony, S. Ehrlich, H. Krieg, A consistent and accurate ab initio parametrization of density functional dispersion correction (DFT-D) for the 94 elements H–Pu, *J. Chem. Phys.* 132 (15) (2010) 154104.
- [47] G. Stefan, E. Stephan, G. Lars, Effect of the damping function in dispersion corrected density functional theory, *J. Comput. Chem.* 32 (7) (2011) 1456–1465.
- [48] A. Klamt, G. Schuurmann, COSMO: a new approach to dielectric screening in solvents with explicit expressions for the screening energy and its gradient, *Journal of the Chemical Society, Perkin Transactions 2* (5) (1993) 799–805.
- [49] Y. Sun, V. Lemaire, J.I. Beltrán, J. Cornil, J. Huang, J. Zhu, Y. Wang, R. Fröhlich, H. Wang, L. Jiang, G. Zou, Neutral mononuclear Copper(I) complexes: synthesis, crystal structures, and photophysical properties, *Inorg. Chem.* 55 (12) (2016) 5845–5852.
- [50] C. Bizzarri, C. Fléchon, O. Fenwick, F. Cacialli, F. Polo, M.D. Gálvez-López, C.-H. Yang, S. Scintilla, Y. Sun, R. Fröhlich, L.D. Cola, Luminescent neutral Cu(I) complexes: synthesis, characterization and application in solution-processed OLED, *ECS J. Solid State Sci. Technol.* 5 (2016) R83–R90.
- [51] J.-L. Chen, X.-F. Cao, J.-Y. Wang, L.-H. He, Z.-Y. Liu, H.-R. Wen, Z.-N. Chen, Synthesis, characterization, and photophysical properties of heteroleptic Copper(I) complexes with functionalized 3-(2'-pyridyl)-1,2,4-triazole chelating ligands, *Inorg. Chem.* 52 (17) (2013) 9727–9740.
- [52] W.L. Jia, T. McCormick, Y. Tao, J.-P. Lu, S. Wang, New phosphorescent polynuclear Cu(I) compounds based on linear and star-shaped 2-(2'-pyridyl)benzimidazolyl Derivatives: syntheses, structures, luminescence, and electroluminescence, *Inorg. Chem.* 44 (16) (2005) 5706–5712.
- [53] M. Mohankumar, M. Holler, E. Meichsner, J.F. Nierengarten, F. Niess, J.P. Sauvage, B. Delavaux-Nicot, E. Leoni, F. Monti, J.M. Malicka, M. Cocchi, E. Bandini, N. Armaroli, Heteroleptic Copper(I) pseudorotaxanes incorporating macrocyclic phenanthroline ligands of different sizes, *J. Am. Chem. Soc.* 140 (6) (2018) 2336–2347.
- [54] G. Gritzner, J. Kuta, REcommendations on reporting electrode potentials in nonaqueous solvents, *Pure Appl. Chem.* 56 (4) (1984) 461–466.
- [55] M. Thelakkat, H.-W. Schmidt, *Adv. Mater.* 10 (1998) 219.
- [56] J. Schneider, H. Jia, J.T. Muckerman, E. Fujita, Thermodynamics and kinetics of CO₂, CO, and H⁺ binding to the metal centre of CO₂ reduction catalysts, *Chem. Soc. Rev.* 41 (6) (2012) 2036–2051.